

Future Technologies – Application of Plasma Devices for Vehicle Systems

D. M. Van Wie

The Johns Hopkins University
Applied Physics Laboratory
Laurel, Maryland, USA

1. ABSTRACT

The application of plasma devices for controlling and enhancing aerodynamic phenomena encountered in atmospheric flight vehicles is actively being investigated by many research groups throughout the world. These devices operate using the generation of plasma within the flowfield, generally through an electrical discharge or injection of an electron beam, and then using either the effects of the energy deposition itself or through application of electrostatic or Lorentz forces to modify the aerodynamic phenomena of interest. Plasma devices are being explored for applications ranging from drag reduction and steering control to boundary layer modification to ignition and combustion system enhancement. Note that since the plasma generation generally operates using electrically controlled phenomena, the frequency response of a control system can be very fast relative to hydraulic and electromechanical systems, so new control strategies can be explored. In the present notes, a variety of plasma flow control devices are described together with a discussion of their potential system-level impacts. High level results are also included from a study conducted by the Johns Hopkins University Applied Physics Laboratory (JHU/APL) titled “Advanced Physics System Study for Future Aerospace Vehicles,” which was performed under the sponsorship of the U. S. Air Force Research Laboratory Propulsion and Power Directorate and Air Vehicles Directorate¹. Within this study, advanced plasma technologies with application to hypersonic flight vehicles were investigated and a system-level study was conducted to demonstrate or bound the potential performance benefits of these technologies.

2. INTRODUCTION

Plasma Aerodynamics is an emerging field wherein plasma discharges are created for the purpose of altering the basic characteristics of the flowfield around a flight vehicle. Experimental and theoretical results have demonstrated phenomena such as reduced drag, reduced heat transfer to bodies, and shock wave modification. Summaries of the early experimental observations have been

Paper presented at the RTO AVT Lecture Series on “Critical Technologies for Hypersonic Vehicle Development”, held at the von Kármán Institute, Rhode-St-Genèse, Belgium, 10-14 May, 2004, and published in RTO-EN-AVT-116.

presented by Mishin² and Klimov et. al.³ and a preliminary look at application areas is provided by Batenin et. al.⁴.

Plasma devices are currently being explored for applications in novel aerodynamic flow control and ignition/combustion enhancement schemes. In the case of aerodynamic flow modification, an air plasma is created using either electrical discharges or injection of an electron-beam. In some devices, the energy deposition that occurs along with the plasma creation is the dominant physical mechanism that allows flow control. In other devices, electrostatic and/or Lorentz forces on the plasma are used to modify the flowfield. For ignition and combustion control, the plasma generation takes place within fuel-air mixtures. For these devices, the thermal energy deposition process is important, but attempts at purposely inducing non-equilibrium chemical reactions to enhance ignition and flameholding are also being pursued.

While plasma devices are being explored for a range of flight speeds, these notes will concentrate principally on their application to flight vehicles operating at supersonic and hypersonic speeds. Many aspects of the technologies under consideration have been investigated for several decades, but the recent resurgence in their interest can be traced to the AJAX vehicle concept, which was developed by the Leninetz Company in St. Petersburg, Russia to support either long-range hypersonic cruise or space access missions^{5,6}. The AJAX vehicle concept incorporates plasma aerodynamic flow control, MHD flow control, power generation, and flow acceleration, and an endothermic fuel reforming process in combination with a basic hydrocarbon-fuel scramjet engine. The AJAX-vehicle technologies provide intriguing system-level synergies for enhancing overall vehicle performance, but the individual technologies also offer the potential for solving a wide range of design problems for hypersonic vehicles. In addressing the plasma devices, the individual technologies are addressed separately with their interdependencies examined to explore a range of potential system application possibilities.

Hypersonic vehicles designed for atmospheric cruise or space access missions share many common technology hurdles as shown schematically in Fig. 1. These include: a) balancing the engine/airframe forces across the speed range; b) controlling the inlet mass capture and observing inlet starting and over-contraction limits; c) minimizing cowl lip drag and heat transfer; d) defining an isolator geometry that meets performance and operability requirements; e) designing fuel injectors which produce adequate mixing with tolerable drag and heat transfer characteristics; f) minimizing transonic drag; g) minimizing nozzle recombination losses; h) controlling boundary layer transition in the inlet; and i) minimizing friction and heat transfer over the airframe. Plasma devices hold the promise to address many of these issues in an efficient manner.

Many of the more promising plasma devices have been considered in a study titled “Advanced Physics System Study for Future Aerospace Vehicles.” The purpose of this study was to investigate advanced plasma technologies with application to high-speed flight vehicles and to conduct system-level studies that demonstrate or bound the potential performance benefits of these technologies. The four primary technology areas considered were plasma aerodynamic flow control, MHD flow control and on-board power generation, plasma-assisted combustion, and advanced endothermic fuels. Some of the high-level results from this study are discussed throughout these notes.

During the initial phase of the system study, specific technologies were selected for further quantitative investigation. A total of 17 technologies in the areas of plasma aerodynamics, MHD flow control and power generation, plasma-assisted combustion, and endothermic fuels were identified and considered. The plasma aerodynamic technologies included: a) plasma jet injection techniques for aerodynamic flow control, b) surface discharges for controlling boundary layers, c) homogeneous volume discharges for flow control, and d) heterogeneous volume discharges for drag reduction. The MHD technologies considered included: a) MHD flow control for inlet mass flow and shock position control, b) MHD flow turning and separation control; c) MHD power generation; d) MHD heat transfer reduction at leading edges; and e) MHD flow control for control surfaces. The plasma-assisted combustion technologies included: a) subcritical microwave discharges; b) fast ionization waves; c) plasma jet injectors; d) pulsed DC discharges with magnetic amplification; and e) a microwave torch. Endothermic fuels, both with and without steam reforming, were considered from the aspect of their energy-balancing capabilities. In these notes, these 17 technologies together with laser-based ignition techniques are discussed.

In the Sections 4 through 7, specific plasma technologies are discussed in the following categories: techniques aimed at increasing engine thrust; techniques aimed at affecting normal and axial forces; techniques aimed at increasing operability; and techniques aimed at improving engine performance. Many of these techniques show potential for improving the performance of flight vehicles, but usually at the expense of additional mass and volume requirements or through requiring power availability from some type of on-board source. Thus, to evaluate the potential benefits of these techniques, several system models needed to be created to provide mass and volume estimates and to allow assessment of on-board power generation requirements. Prior to discussing these individual techniques, some of the general sizing models are discussed that were used in the system impact studies.

3. MODELS

A dual-mission vehicle capable of operating either as a Two-Stage-To-Orbit (TSTO) or a hypersonic cruise vehicle (Fig. 2) was selected as the baseline for assessing the potential impact of plasma technologies. As a TSTO vehicle with a Gross Take-Off Weight (GTOW) of approximately 270,000 kg, this vehicle operates using a hydrocarbon-fueled turboramjet for acceleration to Mach 4.5 followed by a hydrogen-fueled ramjet/scramjet, which accelerates the vehicle to Mach 10 conditions. Following a pull-up zoom maneuver at Mach 10, a rocket-powered second stage is used to boost a small satellite into orbit. As a point of reference, the baseline vehicle uses approximately 13,000 kg of hydrogen fuel for the Mach 4.5-10 acceleration phase. When operating as a dual-fuel hypersonic cruise vehicle, the vehicle accelerates to a Mach 10 cruise condition, where it cruises for approximately one hour. The vehicle uses approximately 41,000 kg of hydrogen for the acceleration and cruise phase of the flight.

In evaluating the engine characteristics with the advanced technologies, a generic hydrogen-fueled engine was designed and used as a baseline. Using an optimized 3-shock forebody design providing shock-on-lip at Mach 10, $q = 0.47$ atm, the engine was designed with a geometric contraction ratio of 16.6, combustor area ratio of 2.0, combustor length-to-entrance height ratio of 10, and an overall engine area ratio of 1.2. For evaluation at hypersonic conditions, the engine cowl height was fixed relative to the body, but a rotating cowl lip was available for modulating the airflow through the engine. Sample values of the baseline engine specific impulse, I_{sp} , and thrust coefficient, C_T , are provided in Fig. 3 for operation at Mach 8, 10, and 12 with equivalence ratios, ER , between 0.2 and 1.2.

Many of the technologies considered require the use of an on-board power generation system. Three types of MHD power-generation systems were considered: a system located in the inlet using non-equilibrium ionization, an MHD system located downstream of the scramjet combustor using a thermally ionized seed material, and a stand-alone JP-7/LOX MHD power generation system. Typical dry mass and consumable mass flows for stand-alone MHD systems were evaluated and the following mass model was developed:

$$M_{MHD} = 0.028P + 0.7 + (0.00086P + 0.0032)t \quad [1]$$

where M_{MHD} is the MHD system mass in tons, P is the generated power in MW, and t is the operating time in seconds. For the inline MHD generator, the following mass model was developed:

$$M_{MHD} = 0.017P + 0.00028Pt \quad [2]$$

A detailed mass model of the inlet-based MHD system was not generated.

Sample power generation mass estimates are provided in Table 1 for 5 MW and 100 MW generation systems for both the 300 s space-access acceleration and 3600-s cruise missions. Note that in all cases, the mass estimate for the inline-MHD power generation system is lower than the auxiliary power system. Also note that the 5 MW system represents less than 10% of the hydrogen fuel mass for both the access-to-space and cruise missions, but the 100 MW system mass is considerably larger than the mass of fuel used in flight. These results indicate that power generation systems capable of producing 5 MW are reasonable, but 100 MW systems will need to have their mass reduced by approximately a factor of 20 in order to be considered viable for the sample missions. Novel techniques for producing low-mass magnets will enable a much broader range of MHD-flow control technologies than are currently feasible.

Several of the technologies evaluated require the use of a non-equilibrium ionization source, which is achieved most efficiently using an electron beam source. Mass and volume requirements for large-scale e-beams were evaluated. For an e-beam system required to ionize the airstream a distance approximately 2 m from the surface, conventional state-of-the-art technology requires a system weighing approximately 1275 kg/m^3 of ionized volume. This 100 keV e-beam system uses an aerodynamic window with pumped aperture and conventional thermionic emitter. It is believed that improvements in the state-of-the-art will allow reduction in the weight to approximately 550 kg/m^3 . The potential of thin-film gallium emitters for flow ionization appears very promising in that mass of the systems is projected to be very low and the integration much more flexible⁷.

4. TECHNIQUES TO INCREASE ENGINE THRUST

Several of the plasma techniques offer as their root benefit an increase in engine thrust by control of the mass flow through the engine. Four basic techniques have been suggested and are illustrated in Fig. 4. The first two techniques represent large-scale inlet flow control technologies where scramjet inlets may benefit from MHD flow control, especially in situations where the inlet is required to operate over a significant range of Mach number and/or angle-of-attack. For conventional scramjet inlets, variable geometry is required to meet the competing requirements of capture flowrate and compression ratio while remaining within operability constraints such as starting limits or shock-wave/boundary-layer interaction limits. MHD flow control for scramjet inlets has been suggested for use in control of the captured flow rate, control of shock positioning, control of compression ratio, and for control of local shock-wave/boundary-layer interactions⁸⁻¹⁵. The Low-High MHD inlet control system is used on a vehicle redesigned for operation at low hypersonic speeds; hence, the inlet is designed for low speed and then the MHD system is used to maintain shock position control as the vehicle is accelerated to higher speeds. This type of system has the advantage that the engine air capture ratio is much higher than the baseline vehicle over the

speed regime where the MHD flow control is used, so higher thrusts are possible. The High-Low MHD Inlet Flow Control System uses the baseline high-speed inlet design, but then uses the MHD flow control to draw additional mass through the engine at speeds below the design speed. Hence, the inlet is designed for high-speed operation and then the MHD system is used to control the flow at lower speeds. The shock-wave/boundary interaction control system is used to prevent boundary layer separation, which allows inlet operation at higher captured mass flows if a variable cowl is used. Finally, a system using a virtual cowl was evaluated¹⁶, which uses off-board energy deposition to direct additional flow through the engine.

Prior to discussing the four specific techniques described above, a brief overview of available background material is provided. In the area of inlet flow turning, Brichkin et. al.⁸ have presented conceptual design level engine cycle calculations that show the effect of inlet flow control on the overall performance of a scramjet engine. Using an engine configuration that was designed for Mach 10 flight, the performance impacts of operating at Mach 6 and 8 were assessed. An ionization region over the external forebody was used to allow control of the flowrate entering the inlet. A relatively low-level engine cycle analysis technique was used to assess the impact of the inlet flow control. Results were provided for the ratio of the magnetoplasmachemical engine (MPCE) as compared to the conventional scramjet for captured flowrate (\dot{m}), specific impulse (I), and thrust (R). Engine performance was calculated as a function of the energy required to operate the ionization system (q_i) divided by the maximum energy that can be extracted from the MHD system (q_{cr}). The results of these calculations indicate that at Mach 6, the use of MHD flow control system can increase the captured flowrate between 25% and 37%, which lead to an increase in specific impulse of 10-12% and a thrust increase between 40 and 50%.

Inlet performance calculations by Vatazhina and Kopchenov^{9,10} have shown that MHD flow control can be used to modify the shock structure in an inlet although operation in a flow expansion mode was shown to be very inefficient. Macheret et. al.¹² have examined the feasibility of using an external MHD system with electron beam ionization for control of a scramjet inlet. Results of their calculations show that the power required for ionization is less than the power generated within the MHD system for inlet operation at a Mach 8, 30 km altitude operating condition. After designing a simple two-shock inlet for operation at Mach 6, calculations showed that shock-on-lip operation could be maintained with MHD flow control at the Mach 8 flight condition. Note that the calculations relied on the flow expansion operating mode. The significant loss in total pressure, which was on the order of 33% for the calculated Mach 8 condition with MHD, would generally not be justified for this type of inlet flow modification.

Both experimental and computational work on the problem of inlet flow control has been conducted by a team of researchers at the Ioffe Physical Technical Institute led by S. Bobashev and

Yu. Golovachov^{14,15}. Experiments have been conducted using a shock tunnel operating with rare gases (krypton, xenon, and argon) to produce an ionized gas that enters a two-shock internal-compression inlet. Segmented electrodes were installed in the upper and lower surface of the inlet, and Helmholtz coils located in the tunnel sidewalls were used to create a magnetic field normal to inlet flow. As seen in the results provided in the right-hand side of Fig. 5, increasing the magnetic field (up to 1.2T) results in a significant increase in the shock wave angles in the inlet. Bobashev et. al. identified regions of weak interaction, unstable interaction, and strong interaction. Using computational magnetogasdynamic interaction models, the basic flow features of the inlet flow control experiments have been reproduced by Golovachov et. al. As seen in the results shown in the left-hand side of Fig. 5, the computed flowfields show the same degree of inlet flow control as was observed in the experiments. These results also showed the large degree of total pressure loss that result with MHD interactions when operating in the flow expansion mode. The analytical and computational work of Bobashev and Golovachov has demonstrated (in rare gases) that inlet flow control can be applied in a controlled manner without destroying the basic wave nature of the inlet compression process. Techniques for generating uniform conductivity in air and for controlled modification of inlet airflows remain to be demonstrated.

4.1 Low-High MHD Flow Control

With the existing studies showing the possibility of large-scale inlet flow control (albeit with large total pressure losses), a more detailed analysis of the four plasma techniques aimed at increasing engine thrust were undertaken. A schematic of the Low-High MHD inlet flow control system is shown in Fig. 6. Preliminary performance calculations indicated that the best performance is achieved with the MHD flow control located as far forward as possible with a narrow interaction region. A large 5-m diameter magnet is located in the forward end of the forebody to produce a 3-T field at the surface of the forebody. A 1D array of e-beam generators is located within the magnet to inject ionizing electrons along the magnetic field lines. The e-beams are sized to generate sufficient ionization at a distance of 2.2-m into the inlet flowfield. Either surface-mounted or instream electrodes are located on either side of the e-beams to collect the transverse current needed for the MHD interaction.

One of the key issues associated with the MHD inlet flow control systems is weight and volume of the magnet. In Ref. 1, several large flat magnets were evaluated for projecting a magnetic field normal to an aerodynamic surface, and the mass model shown in Fig. 7 was developed. This mass model was developed for large toroidal magnets that were designed for a maximum field strength of 7-T in the magnet core, which produces a 3-T field at the surface. The upper range of the mass model corresponds to conventional high-temperature superconducting magnets using steel cryostats and BSCCO-2223 superconducting elements. The lower bound of the mass model

corresponds to projected potential mass reductions and switching to low-temperature superconducting magnets. Note that projected mass of a 5-m diameter magnet is over 100 Ton at the upper limit and 41 Ton at the lower limit, which is much too large for consideration on a 273 Ton GTOW vehicle, so alternate low-mass magnet technologies are needed for any type of large scale inlet flow control system

As described above, the Low-High MHD inlet flow control system was evaluated using an inlet designed for Mach 5 operation with all forebody shocks designed to impinge on the cowl lip at this operating condition. The MHD flow control is used to control the shock position at higher Mach numbers. An example of this control is provided in Fig. 8, which shows flowfield results at Mach 8 from a solution of the 2D Euler equations with a prescribed magnetic field distribution as calculated for the centerline of the magnet shown in Fig. 6. The Mach number and static pressure contours show that the MHD flow control is successful in repositioning the forebody shocks at the cowl lip. The narrow MHD interaction region is seen in the contours of the electron density and static temperature. The results also show that the flow control system operates in a self-sustained mode with the 23.83 MW/m power extracted, more than compensating for the 13.6 MW/m power required for the ionization system.

Despite the issues associated with the magnet mass, the impact of the Low-High MHD inlet flow control system on the baseline engine operation was evaluated at speeds between Mach 5 and 10 and the results are shown in Fig. 9. Results are provided in both a tip-to-tail (T-T) and cowl lip-to-tail (C-T) force accounting system for cases with and without the extra energy extracted from the MHD flow control system added back into the combustor. The results show that the thrust coefficient for the system with the MHD flow control is much higher at Mach 5 than the baseline consistent with the added mass flow, but the thrust advantage drops quickly with increasing speed as the MHD flow control system is used due to intrinsic losses associated with the MHD process. In terms of the tip-to-tail force accounting the engine specific impulse drops continuously as the flight speed increases. With the decrease in C_T and I_{sp} and the increased mass of the magnetic and ionization subsystems, the overall system performance impact of the Low-High MHD flow control system was negative. Thus, the Low-High MHD flow control system does not appear to offer any system-level impact despite its ability to provide shock wave position control within an inlet.

4.2 High-Low MHD Flow Control

The High-Low MHD inlet flow control system attempts to improve on the problems encountered with the Low-High system by retaining the high-speed system design and using the MHD flow control at lower speeds, which should result in smaller losses. Compressive force on the captured airstream can be induced through the use of a diagonal MHD generator within a three-

dimensional inlet. This technique suffers from the need for a large volume ionization source and large magnets, but the engine performance penalties should be lower compared to the Low-High MHD inlet flow control system. At present, detailed performance estimates of the High-Low inlet flow control system have not been generated, but will be reported in future papers.

4.3 MHD Flow Control for Shock-Wave/Boundary-Layer Interactions

Since the large-scale inlet flow control systems have not appeared overly promising, interest in local MHD flow control for inlets arose. The concept behind the local MHD flow control for shock-wave/boundary-layer interaction (SWBLI) is illustrated in Fig. 10. Conventional inlets are often designed for operation against SWBLI constraints to prevent boundary layer separation and the resulting shock-expansion losses and unsteady flow features. With local MHD flow control, it is theorized that boundary layer separation can be avoided by “pumping” the low-momentum flow near the wall through the adverse pressure gradient of the shock interaction. Compared to the global MHD flow control techniques, this local technique has the advantages that the local velocity is low, the boundary layer temperature is high, and the magnetic field and ionized regions are small.

The advantage of the local MHD flow control system was evaluated for an engine concept that employed a rotating cowl. In the baseline engine, the performance of the engine was limited by a “weak-shock” (WS) constraint, which is a boundary layer separation criteria. The results of engine performance calculations with and without the MHD flow control system are shown in Fig. 11. With the MHD flow control system, the engine thrust can be significantly increased at Mach numbers below the design operating condition since the engine cowl can be rotated outward and additional airflow captured. For speeds at or above the design Mach number, the effect of the cowl rotation is minimal as the cowl lip captures uncompressed freestream air. Also note that the engine specific impulse is only slightly changed by the use of the local MHD flow control system. With the added thrust and small weight penalty of the local MHD flow control system, this technique shows promise for a positive impact on the overall hypersonic system performance. Additional research is required on the generation of sufficient air ionization in the near-wall region and the application of the Lorentz force in overcoming the adverse pressure rise of the shock interaction.

4.4 Virtual Cowl

The final technique in this category aimed at increasing thrust is the virtual cowl concept originated by Macheret et. al.¹⁶ In this concept, energy is deposited slightly upstream and outside of the cowl lip to deflect mass flow into the engine. Using inlet performance estimates provided in Ref. 16, the impact of the virtual cowl concept on the engine performance was assessed and the results are shown in Table 2. Results are shown for cases where the deposited energy is extracted from the

engine flowpath or provided by some auxiliary source and the results can be contrasted to the results with an equal amount of energy supplied directly to the combustor. The analyses show that the use of the virtual cowl results in additional captured mass flow, which results in higher thrusts compared to the baseline engine.

In assessing the performance of this concept, one must be careful in addressing the energy generation requirements, which can require significant power levels with a resulting large mass penalty.

5. TECHNIQUES TO ALTER NORMAL/AXIAL FORCES

Plasma Aerodynamics is an emerging field wherein plasma discharges are created for the purpose of altering the basic characteristics of the flowfield around a flight vehicle. As illustrated in Fig. 12, the considered technologies are subdivided into four categories: Plasma Jet Injection, Homogeneous Volume Discharges, Heterogeneous Volume Discharges, and Surface Discharges. Experimental results have demonstrated phenomena such as reduced drag, reduced heat transfer to bodies, and shock wave modification using different types of plasma discharges. Plasma aerodynamics is also being explored as a means of providing normal force enhancement or steering control.

Some of the very early investigations of plasma aerodynamics were conducted in ballistic range tests at the Ioffe Physico-Technical Institute¹⁷. In these experiments, gun-launch projectiles were fired through a gas discharge and the resulting flowfield characteristics were observed. The first experiments conducted at the Ioffe Institute involved the flight of simple shapes (spheres, cones, and stepped cylinders) through steady DC discharges. As seen in Schlieren photographs provided in Fig. 13 from the Ioffe Institute tests, the results showed that the shock standoff distance significantly increased when a sphere was flown through a steady DC discharge region. These experiments were conducted at gas pressures between 40 and 50 Torr with a discharge current density between 20 and 50 mA/cm². The degree of ionization was between 10⁻⁵ and 10⁻⁶ with electron number density in the range of 10¹¹ to 10¹²/cm³ and an electron temperature of 1 to 4 eV. For projectile velocities in the range of 1200 to 2400 m/s, the shock standoff distance was observed to increase by a factor of 1.6 to 2.2 compared to air at the same temperature.

In follow-on tests at the Ioffe Institute, a long region of relatively uniform discharge was used to investigate the drag characteristics for a sphere over a range of flight speeds. The drag coefficient of the sphere was determined as a function of Mach number for tests with and without the discharge¹⁸. In these experiments the air pressure was 15 Torr and the sphere diameter was 15 mm.

The weakly ionized gas ($\alpha \approx 10^{-6}$) was produced using a 440 kHz RF generator. The results showed that the drag coefficient decreased at subsonic speeds and the apparent sonic drag rise occurs at higher velocity. It should also be noted that the drop in drag coefficient at subsonic speeds is inconsistent with a thermal energy deposition model, since an increased temperature will lead to a decreased Reynolds number. These experiments also showed a small drag increase at low supersonic speeds.

5.1 Plasma Jet Injection

Plasma jet injection, wherein plasma is created internal to a model and injected into the flowfield for the purpose of modifying the flowfield, has been investigated by a number of researchers¹⁹⁻²³. Plasma jet injection from a spherically blunted cylinder was shown to reduce drag although unsteady bifurcated flows can result over significant portion of the operating regime. The drag reduction aspects of the plasma jets appear to be principally fluid dynamic in nature. The plasma jets offer the advantage of operation with a high temperature injectant, which allows a given effect to be realized for a smaller amount of injectant. Plasma jet injection has been shown to be energetically efficient in reducing the drag of non-aerodynamic shapes such as spheres. The drag reduction efficiency of this technique increases significantly with increasing Mach number, as the jet injection works to make the flow over the sphere more conical in nature.

The efficiency of the plasma jet injection is much lower for aerodynamic shapes, and plasma jet injection does not appear to be feasible for significantly blunting slender hypersonic vehicles. So, plasma jets appear to offer little advantage for aerodynamic applications where slender shapes are generally used. Plasma jet may offer advantages for application in other flow control situations.

5.2 Homogeneous Volume Discharges

Homogeneous volume discharges, which include a number of plasma generation technologies where the principal purpose is to create a relative uniform volume of plasma in the discharge zone, have also been investigated by a number of researchers^{4,24-33}. For this category, the discharge zone may be located near the body, in the case of discharge between on-board electrodes, or may be located a significant distance from the body, in the case of a laser or microwave discharge system. The available experimental data shows that generation of homogeneous volume discharges can be used for modifying flowfields, including drag reduction. Currently, the drag reduction efficiency of the homogeneous plasma generation systems appears to be similar to that for plasma jet generators. Critical experiments on the effects of off-board energy deposition at high Mach numbers are needed to fully assess the impact of homogeneous volume discharges.

5.3 Heterogeneous Volume Discharges

Heterogeneous volume discharges include a number of plasma generation technologies where the discharge can be very non-uniform both spatially and temporally³⁴⁻⁴³. Heterogeneous discharges can be created by high-frequency discharges, microwave discharges, or injected e-beams. These discharges result in a series of thin streamer-like channels within the flow. The temperatures within the streamers can quickly reach values up to 5000K, which allow interactions with the surrounding airstream. The heterogeneous discharge that has received the most attention is the microwave discharge. Microwave discharges can have either a diffuse or streamer character depending on the pressure of the gas. Kolesnichenko et. al.⁴⁰ have investigated the aerodynamic effects of a microwave discharge upstream of sphere in supersonic flow. The results show that the discharge significantly alters the bow shock structure by inducing high-frequency oscillations in the flowfield.

Leonov et. al.⁴¹ compiled data on the effectiveness of heterogeneous discharges for drag reduction as shown in Fig. 14. The results show that high drag reduction effectiveness is achieved using High-Frequency (HF) heterogeneous discharges for models with low drag coefficients. In these results the actual drag reduction for the most aerodynamic shapes was on the order of 10%. Although these results are very encouraging for improving the aerodynamic efficiency of aerodynamic shapes, the amount of information on this phenomenon is limited.

Soloviev et. al.⁴² conducted a numerical investigation of the interaction of a heterogeneous discharge with the flowfield around a 35° cone. In these calculations, the pulsed discharge was modeled with both constant-pressure and constant-density energy deposition processes. Time-dependent Euler calculations of the flowfield perturbations generated by the discharge were conducted and the resulting effects on the drag were assessed. Drag reductions predicted by the computations increased with freestream Mach number and were dependent on the energy deposition process used to initialize the filaments.

Wilkerson et. al.⁴³ conducted numerical simulations of heterogeneous discharges upstream of a two-dimensional 5° wedge. The effects of filament size, location, energy deposition, and freestream Mach number were investigated with the result that drag reduction could only be achieved in selected cases and the energetic efficiency was low for all cases investigated. In reviewing the results, it was apparent that the level of energy deposition was excessive in that transverse equilibration of the pressure rise following energy deposition was not achieved prior to impingement of the heated zone on the body and a drag increase was obtained in most cases. In the current study, the effects of more modest energy deposition levels on the drag reduction of a 5° wedge were investigated at Mach numbers between 2 and 10.

The drag reduction effectiveness, η_D , is defined as the drag power savings divided by the deposited power:

$$\eta_D = \frac{\int_0^{t_p} \Delta D U_0 dt}{\left(n - \frac{1}{2}\right) t_d L_d \rho C_i \Delta T} \quad [3]$$

where ΔD - change in drag from the baseline no-discharge value, U_0 – freestream velocity, n – number of filaments, t_p – thickness of the discharge filament, L_d – length of discharge filament, ρ - density, C_i – specific heat based on either constant pressure or constant volume depending on the discharge process, and ΔT – temperature rise in the filaments.

Baseline calculations were conducted for a 5° wedge, $n = 7$, $t_d = 0.05$, $Y_d = 0.1$, $L_d = 1$, and $X_d = 0$ with an initial filament temperature 16.7 times the freestream temperature. The drag reduction effectiveness was calculated for Mach numbers between 2 and 10 for both constant-pressure and constant-density energy deposition models (Fig. 15). The constant-pressure model showed increasing η_D with increasing Mach number, which is likely due to the mass removal from the freestream. The constant density model results in negative η_D values (i.e. drag increases), which becomes more negative as the Mach number increases. The effects of reduced energy deposition were evaluated by investigating three additional discharge configurations: a) removal of every other filament; b) calculation of a single filament on the centerline; and c) calculation of the effect of a half-thickness filament on the centerline. Each case was evaluated at Mach numbers of 2, 5 and 10 with $L_d = 1$, $X_d = 10$, and initial filament temperature 16.7 times freestream. The drag reduction effectiveness is shown in Fig. 15 as a function of freestream Mach number for the cases with reduced energy deposition and compared to the baseline case with constant-pressure and constant-density energy deposition models. The results show that as the energy deposition is reduced and concentrated near the centerline of the wedge, the energetic efficiency approaches the trend produced with the constant-pressure deposition model. While the drag reduction effectiveness appears promising, the absolute value of the drag reduction is small for the low energy discharges. The results suggest that the energy should be concentrated on the centerline and located far enough upstream that the pressure equilibration that occurs after energy deposition is completed prior to the heated air impacting the body.

With drag reduction effectiveness approaching 50%, the drag reduction technology becomes competitive with the thrust production efficiency of the scramjet engine. In Table 3, the drag reduction (assuming 10% of the total vehicle drag) and power savings available through the use of a heterogeneous plasma discharge system are presented. For a vehicle accelerating along a $q = 2000$

psf dynamic pressure trajectory, the drag power savings increases between 95 and 161 MW for speeds between Mach 6 and 10. The mass associated with the power generation needed for the discharge system was estimated using the mass models previously described. For a system sized to produce 161 MW of power, the required system mass varied between 46,802 kg for a stand-alone MHD power generator and 39,143 kg for an inline MHD power generation system. For an 82 MW system, the subsystem mass varied between 19,900 kg and 24,500 kg. Again, one can see that the mass associated with power generation is too large for practical systems. System optimization to increase the energetic efficiency of the plasma discharge systems or to decrease the mass of the power generation system can have a significant impact on the viability of the plasma drag reduction systems.

5.4 Surface Discharges

The final plasma aerodynamic technique to be discussed is the surface discharge technique. The use of plasma surface discharges for modifying boundary layer characteristics has been recently investigated⁴⁴⁻⁴⁶ although the available information on surface discharges in supersonic and hypersonic flows is very limited. Stable discharges between surface-mounted electrodes and microwave surface discharges have been explored and reduction of skin friction and delay of boundary layer transition have been observed. Leonov et. al.⁴⁵ have investigated the use of a discharge between surface mounted electrodes to reduce the friction drag of a flat plate. At transonic speeds with a local static pressure of 500 Torr, a 15kW discharge was shown to result in gas heating sufficient to produce a temperature of approximately 1500K. A portion of the flat plate downstream of the discharge was isolated and mounted on a force balance. The drag measurements provided evidence that the friction drag downstream of the discharge is significantly reduced. Microwave surface discharges have also been investigated for the purpose of modifying the boundary layer characteristics in flowfields. Shibkov et. al.⁴⁴ have demonstrated the capability to generate and stabilize a discharge in the presence of a Mach 2 airstream over a length of 15 cm with a cross-sectional area of 1x2 cm². The time variation of the temperature in the discharge has been measured as a function of input temperature with initial heating rates on the order of 50K/ μ s. The very fast gas-heating rate in discharges with high reduced electric fields ($E/n > 100$ Td) has been attributed to the effective excitation of electronically excited states of nitrogen and their subsequent fast quenching. As the pulse power is increased from 35 kW to 175 kW, the gas temperature was found to increase from 500K to 1700K while the vibrational temperature remained nearly constant. Thus, microwave surface discharges provide a means for rapidly heating a boundary layer while a fine control on the resulting temperature can be maintained.

Levin et. al.⁴⁶ have calculated the reduction in surface skin friction coefficient on a flat plate at Mach 3 due to a surface discharge, which was modeled as an energy deposition in a small volume

above the surface. The discharges were shown to impact the skin friction well downstream of the discharge region and energetic efficiencies approaching 50% were calculated for the Mach 3 conditions. No information is available on the effect of increasing Mach number on drag reduction energetic efficiency of surface discharges.

To illustrate the magnitude of the potential savings, the potential reduction in viscous drag and power savings are shown in Fig. 16 for viscous drag reductions between 0 and 50% of the nominal vehicle viscous drag at a Mach 10 condition. Also shown is the deposited power required for this drag reduction for energetic efficiencies between 0.2 and 2. Clearly, increasing the energetic efficiency of the discharge system has a significant effect on the power requirements and system viability. Further techniques to increase the efficiency of the system, through energy deposition optimization and pulsed discharge investigation should be pursued.

6. TECHNIQUES AIMED AT INCREASING OPERABILITY

A number of plasma techniques have been investigated and proposed for increasing the operability of an engine at hypersonic speeds as shown in Fig. 17. The first concept uses MHD flow interactions to reduce heat transfer at a leading edge, while the remaining technologies are aimed at improving and expanding ignition and flameholding limits within an engine. As with all techniques aimed at increasing the operability of an engine, a performance benefit cannot be shown if the baseline engine is assumed to operate as designed; therefore, these techniques are discussed with respect to their ability to be integrated into the baseline engine without significant mass or volume penalties.

Plasma-assisted combustion refers to technologies in which plasma discharges are used for the purpose of enhancing ignition, extending flameholding operability limits, or increasing mixing and combustion efficiencies. The opportunities for plasma-enhanced combustion include: a) minimizing ignition delay time; b) providing robust flameholding; c) shortening the mixing and combustion length; and d) providing stable ignition and burning for external burning systems. For hydrogen-air combustion, the minimization of ignition delay time is principally an issue at high hypersonic speeds where the flow residence time becomes very short. For hydrocarbon fuel-air mixtures, minimization of ignition delay time is especially important at low supersonic speeds where the temperature is low and the natural ignition delay time can be orders of magnitude greater than the flow residence time.

A number of researchers have investigated the role of active radicals and vibrationally and electronically excited states in reducing the ignition delay time of combustible mixtures. Williams

et. al.⁴⁷⁻⁴⁸ have been studying the use of ionized species for the purpose of reducing the ignition delay time of hydrocarbon fuel-air mixtures and the initial results show promise for lowering ignition limits. In all of the various discharge techniques discussed below, a wide spectrum of dissociated, ionized and excited species are created. Each of the plasma ignition techniques offers the promise to increase the operability limits of the scramjet engine. The power, mass, and volume requirements of each technique are small relative to the engines on the baseline vehicles, so small system impacts will accrue for the increased operability.

In the following section, some of the plasma-based techniques that aim to improve vehicle and engine operability are discussed in more detail.

6.1 MHD Flow Control For Reduced Leading Edge Heating

The concept of using MHD effects to reduce heat transfer dates to early hypersonic studies conducted in the 1950s, and a good review of this early effort is provided by Poggie and Gaitonde⁴⁹. In this work, results are also provided from computational and theoretical studies of the hypersonic flow over a hemisphere, which were conducted to investigate the potential use of MHD effects for mitigating the heat transfer at a leading edge. Results show that the stagnation point heat transfer could be reduced by approximately 25% at Mach 5 with a magnetic interaction parameter of 6. A number of other authors have discussed the use of MHD interactions for lowering the peak heat transfer. Batenin et. al.⁴ provided calculations to indicate the potential reduction in heat transfer at a blunt leading edge using current flows along the leading edge to produce a circumferential magnetic field. The resulting $\vec{j} \times \vec{B}$ force leads to a deceleration of the flow approaching the leading edge. Results show that the peak heat transfer rate at the leading edge can be reduced in the presence of a magnetic field. While the MHD flow control for heat transfer mitigation may show benefits, it is likely that this technology will not be competitive for internal cooling and heat pipe approaches to produce robust leading edges for hypersonic systems.

6.2 Laser Discharges for Fuel-Air Ignition

In the area of laser-based ignition of fuel-air mixtures, four main mechanisms exist: laser induced thermal ignition, non-resonant laser induced spark ignition, laser induced photochemical ignition, and resonant laser induced spark ignition⁵⁰⁻⁷¹. Laser induced thermal ignition involves the use of infrared adsorption, typically provided by the 10.6 micron output of a CO₂ laser, to excite specific molecular vibrational levels within the fuel/oxidizer mixture. The excited molecules rapidly dissipate the energy and thermally heat the gas to the point of thermal ignition. To date, this method has only been effective in stationary gaseous, liquid or solid propellant fuel due to the long times

required to couple the thermal energy into the propulsive media. Non-resonant laser induced spark ignition involves the use of a high power, pulsed laser to produce large electric field strengths, causing local gas breakdown. This breakdown results in a spark discharge that generates a high-temperature plasma which, in turn, ignites the gas. This is the method of laser energy deposition that most closely resembles the typical electric spark discharge based ignition.

Both the third and fourth mechanisms listed above for laser-based ignition require the absorption of specific wavelength optical energy to photo-dissociate or photo-ionize specific species of either fuel or oxidizer. In laser-induced photochemical ignition, either infrared or ultraviolet multi-photon absorption is employed to photo-dissociate specific molecular species (fuel or oxidizer) and, therefore, create a highly reactive gas mixture capable of ignition and sustained combustion. The fourth method for the laser ignition of mixed fuel-air is the most recent method used for producing laser-based ignition. It is, basically, a combination of photochemical ignition and non-resonant spark ignition. It is termed resonant laser-induced spark ignition and involves the use of tuned UV light to produce molecular and/or atomic resonances resulting in the efficient multiphoton ionization production of seed electrons to initiate gas breakdown. The laser power requirements for this method of ignition are the lowest, <2 mJ. However, precise tuning of laser frequencies deep in the UV is required.

One of the earliest studies performed in the area of laser-induced ignition was an experimental study of laser ignited plasmas in quiescent hydrogen gas using a type of non-resonant spark ignition. Van Zandt et. al.⁵⁰ performed these plasma experiments using a dual laser scheme. A pulsed CO₂ laser was used to create a spark within a quiescent hydrogen gas, producing a high energy density plasma. A second continuous wave (CW) CO₂ laser was then focused coincident to the pulsed laser's focal point, maintaining the high-energy plasma which can be expanded through a nozzle for thrust production (no actual ignition of a fuel-air mixture took place). The pulsed laser provided an energy of 7 joules with a 150 ns pulse length (46 MW) and the CW laser provided 30 kW of power. Another early experiment in laser ignition was performed Chou et. al.⁵⁸. This group reported on the use of metallic needles at the focal point of the laser energy to enhance, via surface breakdown, the coupling of the laser energy into quiescent and low velocity gaseous media during non-resonant spark ignition. Syage et al.⁵⁶ investigated flame propagation initiated by laser-induced sparking in premixed, quiescent H₂/air, and Spiglanin et al.⁶⁷ imaged very early flame kernel growth for the laser spark ignition of quiescent and low velocity H₂/O₂/Ar mixtures.

Beginning in the 1980's considerable, work was reported using photochemical laser ignition of gaseous fuel/oxidizer mixtures. Lavid et al.^{51,62} used a F₂ excimer laser (157 nm) and an ArF excimer laser (193 nm) to reliably ignite H₂/O₂ mixtures. Lucas et al.⁵⁵ employed a KrF laser (248 nm) to photolyze an additive O₃ to ignite H₂/O₂, CH₄/O₂ and C₃H₈/O₂ mixtures. Chou and

Zukowski⁵⁸ also employed an ArF excimer laser to photolyze another additive, NH_3 , to ignite H_2/O_2 , H_2/air and CH_4/O_2 mixtures.

Forch et. al.^{54,63} found a strong wavelength dependence in the amount of incident laser energy required to ignite a slowly flowing H_2/O_2 mixture. It was found that the focused UV laser not only caused photodissociation of O_2 into O atoms, but also, when tuned to O-atom resonance, required a minimum energy to ignite the gas. The new mechanism was termed resonant spark ignition. In subsequent experiments employing this laser ignition mechanism, the ignition of a mixture of C_2H_2 and air was accomplished with as little as 0.25 mJ of incident laser energy using an ArF excimer laser operating at 193 nm wavelength. The ignition of H_2/O_2 , flowing from a water-jacketed burner at 103 cm/sec was achieved with 0.6 mJ at a wavelength of 225.6 nm. The ignition properties of H_2/O_2 and $\text{H}_2/\text{N}_2\text{O}$ flows at atmospheric pressure using both resonant and non-resonant spark ignition were compared. The non-resonant spark ignition approach required ~20 mJ of laser power for ignition while the resonant approach required as little as 0.55 mJ of laser power indicating the energy advantage of using the resonant ignition system.

As seen above, laser-based ignition with gaseous fuel (mainly CH_4 and H_2) in quiescent or slow moving oxidizer has received considerable laboratory attention. However, the ignition of liquid fuel has been, for the most part, ignored.

Of the four mechanisms, resonant spark ignition has enjoyed the most investigation and success in the laboratory despite being the newest laser ignition mechanism investigated. It is the most energy efficient mechanism, with orders-of-magnitude energy requirement reductions in most cases. Of the three remaining mechanisms, non-resonant spark ignition is the most viable option. Thermal ignition has unacceptably long ignition times for high velocity combustion. Also, thermal ignition is performed with IR wavelengths which are not easily transmitted through either conventional optics or fiber optics and typical CO_2 lasers are bulky, fragile, and expensive. Photochemical ignition employs lasers similar to those required for resonant spark ignition while requiring more energy.

Three new non-resonant laser-based ignition approaches using liquid fuel sprayed into flowing air were independently developed and patented⁷¹. The most effective and reliable of these techniques is similar to the dual-laser based experiments performed by Van Zandt, et. al.⁵⁰. Named dual-pulse ignition, this ignition scheme uses a short, higher powered pulse (10 ns, ~50mJ) from a Nd:YAG laser to generate a plasma and a second long, low-power pulse (200 ns, <50mJ) from a Cr:LiSAF laser to sustain the plasma until ignition occurs. Here, reliable ignition was found over a wide range of fuel compositions using up to 50% less laser power than conventional laser-induced spark ignition. The lower energy requirements in the dual-pulse ignition scheme (up to a factor of 2)

avoid problems with detonation and spark blow-out sometimes encountered at extreme off-design conditions in single-pulse laser systems.

Dual-pulse ignition, while being the most reliable and energy efficient of the two non-resonant laser ignition schemes, requires both a short pulse laser (~10 ns) and an additional long pulse laser (~200 ns) operating in the visible to near IR wavelengths. In order to simplify the ignition system for the experimentation described herein, a novel single-pulse laser ignition scheme was designed with the goal of mimicking the dual-pulse ignition mechanism. A single laser, pulsed at 5 Hz is focused onto a wall-mounted flint or graphite target. The action of the focused beam against the target surface produces a small plasma plume that extends centimeter distances from the target surface. The sustained laser energy, in turn, maintains the plasma for up to 100 μ s. The sustained plume allows the generation of several nearly coincident flame kernels.

Thompson et. al.⁷⁰ investigated the use of a non-resonant laser ignition systems within a hydrocarbon-fueled scramjet combustor. A laser-beam was introduced into a combustor chamber such that it impacted a target located in a cavity region behind the main combustor fuel injectors. Using JP-7 fuel at Mach 6 conditions, the laser ignition system successfully lit the cavity flameholder region.

6.3 Subcritical Microwave Ignition

Subcritical microwave discharges involve the use of microwave energies at power levels below that required to initiate a discharge in free space. For this type of system, some auxiliary initiation process must be used such as a laser initiation system or some type of field concentrating device. Microwaves offer the advantages that they can be efficiently created using a compact system, the discharge can occur over a relatively large volume, and significant undercritical factors are achievable resulting in good power efficiency. Both Khodataev et. al.^{72,74} and Timofeev et. al.⁷³ have investigated the subcritical microwave discharge for ignition of hydrocarbon-fuel/air mixtures. Once initiated, the discharge expands to fill the volume where the field strength is adequate to support the discharge, so a large volume of plasma is produced. Since the discharge has a streamer characteristic, the energy is deposited into a fairly narrow portion of the volume, so the ignition system is energetically efficient. Khodataev et. al.⁷⁵ have successfully ignited propane/air mixtures using a subcritical microwave discharge. The discharge can be either separating, where it propagates toward the source of the radiation to either fill the volume where the field strength is sufficient to support a propagating discharge or fill the volume to the extent that can be completed within the duration of the microwave pulse, or attached, where the discharge remains attached to the initiating source.

6.4 Pulsed Transversal Discharges

The pulse transversal discharge has also been investigated by Timofeev et. al.^{76,77}. The transversal discharge consists of short duration pulses between electrodes that exist for time durations between tens and hundreds of microseconds. Measurements of the discharge characteristics have shown that the discharge is significantly affected by the supersonic flow with the production of a highly non-equilibrium mixture. These discharges have been shown to be useful for igniting cold propane-air mixtures at Mach 2 conditions.

6.5 Fast Ionization Waves

The fast ionization wave has been explored by Starikovskii et. al.^{78,79}. This discharge consists of very short duration pulses (on the order of nanoseconds) at very high specific electric field strength (E/n), which creates a highly non-equilibrium starting point for the ignition process. Starikovskii has shown analytically and experimentally, that the pulsed nanosecond discharge can significantly shorten the ignition delay time of methane-air mixtures at temperatures on the order of 1200K. At higher temperatures, the nanosecond discharges are ineffective at decreasing the ignition delay time, where thermal processes dominate.

6.6 Plasma Jet Injectors

Plasma jet injectors also offer the potential for enhancing ignition through the creation of excited species and radicals with subsequent injection of this mixture into a fuel-air region. One particular type of plasma jet injector, which has been investigated by Timofeev et. al.⁷³ is referred to as the plasmadynamic injector. In this type of device, a large discharge current erodes a portion of the fuel creating a plasma, which is then accelerated to high speeds using a self-induced magnetic field. This type of injector has been shown to inject the plasma at very high velocities, which translates into large cross-stream penetration distances resulting in significant cross-flow penetration.

6.7 Pulsed DC Discharges and Microwave Torches

Pulsed DC discharges and microwave torches have also been investigated. Leonov et. al.⁸⁰ have investigated a pulsed DC discharge from wall mounted electrodes for ignition is non-uniform kerosene-air mixtures. This type of discharge creates hot filaments that interact with the chemical energy release of combustion to generate instabilities in the flow, which produce rapid movement and mixing of the discharge filaments. Kosyiy et. al. have investigated the characteristics of a microwave torch as a potential ignition system.

7. TECHNIQUES AIMED AT INCREASSING ENGINE PERFORMANCE

The three final plasma techniques discussed are aimed at increasing engine performance as illustrated in Fig. 18: inlet laminar flow control; plasma-assisted mixing from a heterogeneous discharge; and plasma-assisted mixing with MHD augmentation. Each of these techniques offers the potential to improve the efficiency of the engine leading to an increase in engine specific impulse.

7.1 Inlet MHD Laminar Flow Control

The concept behind the inlet laminar flow control system extends from the observation that boundary layer transition in most inlets can be traced to either Görtler instabilities created in the concave turning of the compression surface or instabilities in the separated shear layer resulting from laminar boundary layer separation. As illustrated in Fig. 19, a localized MHD-flow control system can potentially be used to stabilize these transition sources and extend the laminar region in the hypersonic inlet. Sample engine performance calculations were conducted to assess the impact of a laminar flow inlet for Mach numbers between 6 and 12 for flight at dynamic pressures of 1000 and 2000 psf. The resulting engine Isp and C_T are shown in Fig. 20 where modest improvements are seen. Potentially more significant results from the inlet laminar flow control system concern the mass of the thermal protection system, which would be lower with the laminar flow control system. To date, experimental demonstrations of an inlet laminar flow control system have not been conducted.

7.2 Plasma and MHD Driven Mixing Enhancement

The use of plasma discharges and MHD-driven mixing offers the potential to shorten the mixing and combustor length within a scramjet engine, which will have significant vehicle performance implications. In these techniques, plasma discharges are created within a fuel-air mixture. The strong thermal non-uniformities created can couple with the combustor fluid dynamics to result in strong vorticity production and internal jetting within the combustor flowfield, which will lead to enhanced mixing.

MHD driven mixing schemes rely on the use of the Lorentz force to enhance the macroscopic mixing. As an illustration of an MHD mixing augmentation system, Biturin et. al.⁴ have investigated the use of a pulsed arc-discharge coupled to a magnetic field. The results show significant driven motion in the plasma channel, which can lead to an increase in mixing effectiveness. Natural instabilities often exist within MHD driven flows, which can be used in the mixing enhancement schemes. The impact of the MHD forces on the microscopic mixing are not well understood at this time.

To date, little quantitative information exists concerning plasma and MHD mixing enhancement schemes, but basic research continues.

8. SUMMARY

Plasma devices offer the potential to provide new forms of flow control for future flight vehicles. In this set of notes, 18 specific technologies that use plasma generating devices have been described. These technologies are as follows:

Techniques Aimed at Increasing Thrust:

1. Low-high MHD inlet flow control
2. High-low MHD inlet flow control
3. Shock-wave/boundary-layer interaction control
4. Virtual cowl

Techniques Aimed at Altering Normal/Axial Forces

5. Homogeneous volume discharges for off-board flow control
6. Heterogeneous volume discharges for drag reduction and vorticity production
7. Surface plasma discharges for reducing skin friction and controlling transition
8. Plasma jet injection for shock position control around leading edges

Techniques Aimed at Increasing Operability

9. MHD heat transfer reduction at leading edges
10. Laser ignition techniques
11. Microwave discharges for fuel ignition
12. Microwave torch ignition and flameholding
13. Pulsed DC Discharge ignition and flameholding
14. Fast ionization wave discharges for fuel ignition
15. Plasmadynamic injector for ignition and flameholding

Techniques Aimed at Increasing Engine Performance

16. Inlet laminar flow control
17. Plasma assisted mixing with heterogeneous discharge
18. Plasma assisted mixing with MHD augmentation

After assessing these technologies, several general trends emerged as follows

1. The mass and volume requirements of the magnet needed for large-scale inlet flow control technique are currently too large for practical applications. A two-order-of-magnitude

reduction in conventional superconducting magnet mass will be required to achieve performance benefits.

2. The mass and volume requirements for the power generation system has a first-order impact on the viability of the drag reduction schemes, so efficient generation of on-board power will be required.
3. Both experimental and numerical simulations have demonstrated promising ranges of drag reduction energetic efficiencies, which begin to have positive system impacts with a light-weight power generation subsystem.
4. MHD heat transfer reduction at leading edges appears to offer little system improvement.
5. Plasma assisted ignition and flameholding system offer increased system operability for small mass, volume, and power penalties.
6. Plasma assisted mixing with or without MHD offers the potential to significantly shorten scramjet combustors.

The development and application of plasma devices is still in an early embryonic phase and significant additional research is required to fully understand their potential and detailed system benefits.

9. ACKNOWLEDGEMENTS

The Advanced Physics Systems Study for Future Aerospace Applications was sponsored by the Propulsion & Power and Air Vehicle Directorates at the Air Force Research Laboratory. In conducting the project, The Boeing Corporation was sub-contracted to gain their perspective as an airframe manufacturer early in the technology assessment and to create preliminary designs for conceptual systems evaluated during the second phase. Textron, SureBeam, Princeton University, Everson, and CCRE also assisted in developing component models. Joseph Silkey coordinated the activities of The Boeing Company. Drs. Sergey Macheret and Michail Shneider of Princeton University supplied the CFD results of the inlet flow control system. Dr. Bo Cybyk and Jordan Wilkerson supplied the CFD computations of the heterogeneous discharge over the two-dimensional wedge.

10. REFERENCES

1. “Research Issues Resulting from an Assessment of Technologies for Future Hypersonic Aerospace Systems, D. M. Van Wie, D. J. Risha, and C. F. Suchomel, AIAA-2004-1257, January 2004.

2. “Sound and Shock Waves in a Gas Discharge Plasma,” G. I. Mishin, Proceedings of the 1st Workshop on Weakly Ionized Gases, Colorado, June 1997.
3. “Review: Plasma Formation and Plasma Aerodynamics,” A. Klimov, S. Leonov, V. Bityurin, V. Brovkin, V. Bychkov, V. Gromov, Yu. Kolesnichenko, A. Lutsky, and Yu. Serov,” Task 3, Milestone 1 Report , JHU/APL contract 785461, 1999.
4. “EM Advanced Flow/Flight Control,” V. M. Batenin, V. A. Bityurin, A. N. Bocharov, V. G. Brovkin, A. I. Klimov, Yu. F. Kolesnichenko, and S. B. Leonov, AIAA-2001-0489, January 2001.
5. “The Application of MHD Systems in Hypersonic Flight Vehicle,” V. L. Fraishtadt, A. L. Kuranov, and E. G. Sheikin, Technical Physics, Col. 43, No. 11, 1998.
6. “AJAX: New Directions in Hypersonic Technology,” E. P. Gurianov and P. T. Harsha,” AIAA-96-4609, 1996.
7. “Field Electron Emitter for Air Ionization in a Supersonic Flow,” S. V. Bobashev, Yu. P. Golovochoy, V. N. Shrednik, D. M. Van Wie, The Fourth Workshop on Magnetoplasma Aerodynamics for Aerospace applications, Moscow, April 2002.
8. “Utilization of MHD Systems on Hypersonic Vehicles,” D. I. Brichkin, A. L. Kuranov, E. G. Sheikin, Perspectives of MHD and Plasma Technologies in Aerospace Applications, Moscow, March, 1999.
9. “Numerical Investigation of Hypersonic Inviscid and Viscous Flow Deceleration by Magnetic Field,” A. Vatazhin, V. Kopchenov, and A. Gouskov, Perspectives of MHD and Plasma Technologies in Aerospace Applications, Moscow, March, 1999.
10. “Estimation of Possibility of Use of MHD Control in Scramjet,” V. Kopchenov, A. Vatazhin, and O. Gouskov, AIAA-99-4971, 3rd Weakly Ionized Gas Workshop, Norfolk, November 1999.
11. “Problem of Hypersonic Flow Deceleration by Magnetic Field,” A. B. Vatazhin and V. I. Kopchenov, Chapter 14 in Scramjet Propulsion, E. T. Curran and S. N. B. Murphy (eds.), Volume 189 in AIAA Progress in Aeronautics and Astronautics Series, 2000.
12. “External Supersonic Flow and Scramjet Inlet Control by MHD With Inlet Control by MHD with Electron Beam Ionization,” S. A. Macheret, M. N. Shneider and R. B. Miles, AIAA-2001-0492, January 2001.
13. “MHD Control by Expternal and Internal Flows in Scramjets under ‘AJAX’ Concept,” A. L. Kuranov and E. G. Shieken, AIAA-2003-0173, Jan. 2003.
14. “Experiments on MHD Control of Attached Shocks in Diffuser,” S. V. Bobashev, A. V. Erofeev, T. A. Lapushkina, S. A. Poniaev, R. V. Vasil-eva, D. Van Wie, AIAA-2003-0169, Jan. 2003.
15. “MHD Control of the Separation Phenomenon in a Supersonic Xenon Plasma Flow. I,” S. V. Bobashev, N. P. Mende, V. A. Sakharov, D. Van Wie, AIAA-2003-0168, Jan. 2003.
16. “Scramjet Inlet Control by Off-Body Energy Addition: A Virtual Cowl,” S. O. Macheret, M. N. Shneider, and R. B. Miles, AIAA-2003-0032, Jan. 2003.

17. “Flow Around a Sphere Moving Supersonically in a Gas Discharge Plasma,” G. I. Mishin, Yu. L. Serov, and I. P. Yavor, *Sov. Tech. Phys. Lett.*, Vol. 17, No. 6, June 1991, pp. 413-416.
18. “Ballistic Studies of the Aerodynamic Drag on a Sphere in Ionized Air,” A. P. Bedin and G. I. Mishin, *Tech., Phys. Lett.*, Vol. 21, No. 1, January 1995, pp. 5-7.
19. “Experimental And Theoretical Study Of The Possibility Of Reducing Aerodynamic Drag By Employing Plasma Injection,” Yu.Ch. Ganiev, V.P. Gordeev, A.V. Krasilnikov, V.I. Lagutin, V.N. Otmennikov, A.V. Panasenko, *Proceedings of the 2nd Weakly Ionized Gas Workshop*, Norfolk, April, 1998.
20. “Effect of Plasma Jet Characteristics on Supersonic Cone-Cylinder Drag,” Yu. Babichev, A. Krasilnikov, A. Panasenko, and G. Sipachev, *AIAA-99-4881*, 3rd Weakly Ionized Gas Workshop, Norfolk, November 1999.
21. “Effect of Plasma Jet Characteristics on Supersonic Cone-Cylinder Drag,” Ju. Babichev, A. Krasilnikov, A. Panasenko, and G. Sipachev, *AIAA-99-4881*, November 1999.
22. “Influence of Counterflow Plasma Jet on Supersonic Blunt Body Pressures,” N. D. Malmuth, V. M. Fomin, A. A. Maslov, V. P. Fomishev, A. P. Shashkin, T. A. Korotaeva, A. N. Shiblyuk, and G. A. Pozdnyakov, *AIAA-99-4883*, 3rd Weakly Ionized Gas Workshop, Norfolk, November 1999.
23. “Hypersonic Flow over a Blunt Body with Plasma Injection,” J. S. Shang, J. Hayes, and J. Menart, *AIAA-2001-0344*, January 2001.
24. “Plasma Generators for Wind Tunnel Tests,” A. I. Klimov and S. B. Leonov, *AFRL-PR-WP-TR-1998-2055*, January 1998.
25. “Studies of Oblique Shock Waves in Weakly Ionized Non-Equilibrium Plasmas,” S. Merriman, I. Adamovich, and J. W. Rich, *AIAA-99-4823*, November 1999.
26. “Supersonic Non-equilibrium Plasma Wind Tunnel Measurements of Shock Modification and Flow Visualization,” R. Yano, V. Contini, E. Plonjes, P. Palm, S. Merriman, S. Aithal, I. Adamovich, W. Lampert, V. Subramaniam, and J. W. Rich, *AIAA Journal*, Vol. 38, No. 10, October 2000, PP. 1879-1888.
27. “Investigation of a Laser-Supported Directed-Energy ‘Air Spike’ in Mach 6.2 Air Flow – Preliminary Results,” M. A. S. Minucci, P. P. G. Toro, J. B. Chanes, A. L. Pereira, H. T. Nagamatsu, and L. N. Myrabo, *AIAA-2001-0641*, January 2001.
28. “Energy Deposition in Supersonic Flows,” R. G. Adelgren, G. S. Elliot, D. D. Knight, A. A. Zheltovodov, and T. J. Breutner, *AIAA-2001-0885*, January 2001.
29. “Thermal Phenomena and Plasma Aerodynamics,” M. N. Kogan, *Proceedings of the 2nd Weakly Ionized Gas Workshop*, Norfolk, April, 1998.
30. “Blunt Body Wave Drag Reduction Using Focused Energy Deposition,” D.W. Riggins, H.F. Nelson, E. Johnson, *Proceedings of the 2nd Weakly Ionized Gas Workshop*, Norfolk, April, 1998.
31. “Effect of a Local Energy Supply Region on 3D Flow Around a Cone,” V. A. Levin and L. V. Terent’eva, *Fluid Dynamics*, Vol. 34, No. 3, 1999, pp. 388-394.

32. “Some Recent Results in Aerodynamic Applications of Flows with Localized Energy Addition,” G. G. Chernyi, AIAA-99-4819, November 1999.
33. “Dynamic Effects for Supersonic Flows over Space-Distributed Energy Sources of High Power Gases,” P. Yu. Georgievsky and V. A. Levin, 2nd Workshop on Magneto- Plasma-Aerodynamics in Aerospace Applications, Moscow, April 2000.
34. “Influence of a HF Corona Plasma Structure on Drag Reduction of Axial-Symmetric Body in a Supersonic Airflow,” V. Bityurin, A. Klimov, S. Leonov, A. Pashina, V. Skvortsov, and T. Cain, AIAA-99-4856, November 1999.
35. “Influence of a Corona Discharge on the Supersonic Drag of an Axisymmetric Body,” A. Klimov, S. Leonov, A. Pashina, V. Skvortsov, T. Cain, and B. Timofeev,” AIAA-99-4856, November 1999.
36. “Supersonic Body Drag Reduction During Forebody Filamentary Discharge Temporal Evolution,” V. R. Soloviev, V. M. Krivtsov, A. M. Konchakov, and N. D. Malmuth, 2nd Workshop on Magneto- Plasma-Aerodynamics in Aerospace Applications, Moscow, April 2000.
37. “Drag Force Coefficient in the Presence of Heterogeneous Relaxation,” E. Ya. Kogan and I. P. Zavershinsky, 2nd Workshop on Magneto- Plasma-Aerodynamics in Aerospace Applications, Moscow, April 2000.
38. “Parameters of Plasma in the Resonant Channel Microwave Streamer Discharge of High Pressure,” L. P. Grachaev, I. I. Esakov, and K. V. Khodataev, 2nd Workshop on Magneto- Plasma-Aerodynamics in Aerospace Applications, Moscow, April 2000.
39. “Dynamic of a Single-Electrode HF Filament in Supersonic Airflow,” S. Leonov, B. Bityurin, and Yu. Kolesnichenko, AIAA 2001-0493, January 2001.
40. “Optimization of MW Plasma Influence on Aerodynamic Characteristics of Body in Airflow,” Yu. Kolesnichenko, EOARD-IVTAN-ISTC Project 1779P, April 2001.
41. “Effectiveness of Plasma Jet Effect on Bodies in Airflow,” S. Leonov, V. Nebolsin, and V. Shilov, Perspectives of MHD and Plasma Technologies in Aerospace Applications, Moscow, March, 1999.
42. “Simulation of Supersonic Body Drag Reduction Produced by Forebody Filamentary Plasmas,” V. Soloviev, V. Krivtsov and A. Konchakov, and N. Malmuth, AIAA-2001-2727, June 2001.
43. “Numerical Assessment of Heterogeneous Plasma Discharge Effects on Supersonic Forebody Drag,” J. T. Wilkerson, D. M. Van Wie, and B. Z. Cybyk, AIAA-2003-0526, Jan. 2003.
44. “Surface Microwave Discharge in Supersonic Airflow,” V. M. Shibkov, A. V. Chernikov, V. A. Chernikov, A. P. Ershov, L. V. Shibkova, I. B. Timofeev, D. A. Vinogradov, A. V. Vaoskanyan, 2nd Workshop on Magneto- Plasma-Aerodynamics in Aerospace Applications, Moscow, April 2000.
45. “Influence of Surface Electrical Discharge on Friction of Plate in Subsonic and Transonic Airflow,” S. Leonov, V. Bityurin, N. Savischenko, A. Yuriev, and V. Gromov, AIAA-2001-0640, January 2001.

46. “Skin Friction Reduction by Energy Addition into a Turbulent Boundary Layer,” V. A. Levin and O. B. Larin, AIAA-2003-0036, Jan. 2003.
47. “Progress on the Investigation of the Effects of Ionization on Hydrocarbon/Air Combustion Chemistry,” S. Williams, A. J. Medley, S. T. Arnold, P. M. Bench, A. A. Viggiano, R. A. Morris, L. Q. Maurice, and C. D. Carter, AIAA-99-4907, 3rd Weakly Ionized Gas Workshop, Norfolk, November 1999.
48. “Reaction and Thermochemistry of Alkyl Ions, C_nH_{2n+1} ($n=1-8$) in the Gas Phase,” S. Williams, T. Miller, W. Knighton, A. Midey, S. Arnold, A. Viggiano, and C. Carter, AIAA-2003-0704, Jan. 2003.
49. “Computational Studies of Magnetic Control in Hypersonic Flow,” J. Poggie and D. V. Gaitonde, AIAA-2001-0196, January 2001.
50. Van Zandt, D. M., T. D. McCay, and R. H. Eskridge, “An Experimental Study of Laser Supported Hydrogen Plasmas,” AIAA Paper 84-1572, June 1984.
51. Lavid, M., J. G. Stevens, *Combustion and Flame*, Vol 60, pp. 195-202, 1985.
52. Forch, B. E., and Miziolek, A. W., “Photochemical Ignition Studies. II. Oxygen-Atom Two-Photon Resonance Effects,” US Army Ballistic Research Laboratory Technical Report BRL-TR-2740, 1986.
53. Forch, B. E., and Miziolek, A. W., “Photochemical Ignition Studies. III. Ignition by Efficient and Resonant Multiphoton Photochemical Formation of Microplasmas,” US Army Ballistic Research Laboratory Technical Report BRL-TR-2809, 1987.
54. Forch, B. E., and A. W. Miziolek, *Combustion Science and Tech.*, Vol. 52, pp. 151-159, 1987.
55. Lucas, D., D. Dunn-Rankin, K. Horn, and N. J. Brown, *Combustion and Flame*, Vol. 69, pp. 171-184, 1987.
56. Syage, J. A., E. W. Fournier, R. Rianda, and R. B. Cohen, “Dynamics of Flame Propagation Using Laser-Induced Spark Initiation: Ignition Energy Measurements,” *Journal of Applied Physics*, Vol. 64, No. 3, pp. 1499-1507, 1988.
57. “Combustion Enhancement by Plasma Jet Ignition in Lean Mixtures,” S. Ono, E. Murase, K. Hanada, and K. Fujiki, *JSME International Journal, Series II*, Vol. 32, No. 4, 1989.
58. Chou, M.-S., and T. J. Zukowski, *Combustion and Flame*, Vol. 87, pp. 191-202, 1991.
59. “Transverse Discharge in a Supersonic Air Flow,” L. P. Grachev, N. N. Gritsov, G. I. Mishin, A. A. Kharlamov, and K. V. Khodataev,” *Sov. Phys. Tech. Phys.*, Vol. 36, No. 9, September 1991, pp. 1073-1075.
60. Ronney, P. D., “Laser versus conventional ignition of flames,” *SPIE-Proceedings of the International Society for Optical Engineering*, Vol. 1862, pp. 2-22, 1993.
61. Chou, M.-S., F. E. Fendell, and H. W. Behrens, “Theoretical and Experimental Studies of Laser-Initiated Detonation Waves for Supersonic Combustion,” *SPIE-Proceedings of the International Society for Optical Engineering*, Vol. 1862, 1993, pp. 45-58.

62. Lavid, M., D. Zhou, and Y.-C. Li, "Ignition of Kerosene Vapor/Air Mixtures with an ArF Excimer Laser," 31st JANNAF Combustion Subcommittee Meeting, Volume III, Lockheed Missiles and Space Company, Sunnyvale, CA, CPIA Publication 620, 17-21 October, 1994.
63. Forch, B. E., "Resonant Laser Ignition of Reactive Gases," *SPIE-Proceedings of the International Society for Optical Engineering*, Vol. 2122, pp. 118-128, 1994.
64. Lavid, M., D. Zhou, and Y.-C. Li, "Ignition of Kerosene Vapor/Air Mixtures with an ArF Excimer Laser," 31st JANNAF Combustion Subcommittee Meeting, Volume III, Lockheed Missiles and Space Company, Sunnyvale, CA, CPIA Publication 620, 17-21 October, 1994.
65. Lavid, M., Y. Nachshon, S. K. Gulati, and J. G. Stevens, *Combustion Sci. and Tech.*, Vol. 96, pp. 231-245, 1994.
66. Lavid, M., D. Zhou, and Y.-C. Li, "Ignition of Jet A with KrF and ArF Excimer Lasers," 32nd JANNAF Combustion Subcommittee Meeting, Volume III, NASA Marshall Space Flight Center, Huntsville, AL, CPIA Publication 631, 23-27 October, 1995.
67. Spiglanin, T. A., A. McIlroy, E. W. Fournier, R. Rianda, R. B. Cohen, and J. A. Syage, "Time-Resolved Imaging of Flame Kernels: Laser Spark Ignition of H₂/O₂/Air Mixtures," *Combustion and Flame*, Vol. 102, No. 3, pp. 310-328, 1995.
68. Medoff, L. D., and A. McIlroy, "Laser-Induced Spark Flameholding in Supercritical, Subsonic Flow," *Journal of Propulsion and Power*, Vol. 13, No. 6, pp. 721-729, Nov.-Dec. 1997.
69. "Some Laws Governing Laser Beam Ignition of an Ethylene Stream in Air," G. I. Kozlov, *Tech. Phys. Letters*, Vol. 23, No. 12, December 1997.
70. "Laser Ignition of Liquid Hydrocarbon Fuels in a Scramjet Combustor," M. W. Thompson, A. L. Wesner, R. Oldenberg, and J. Early, Proceedings of the 36th JANNAF Combustion Subcommittee/Airbreathing Propulsion Subcommittee Meeting, October 1998.
71. Multiple Laser Pulse Ignition Method and Apparatus, US Patent 5,756,924, May 26, 1998; Laser Ablation Based Fuel Ignition, US Patent 5,769,621, June 23, 1998; Laser Preheat Enhanced Ignition, US Patent 5,876,195, March 2, 1999.
72. "Experimental Investigation of a Possibility of a MW Streamer Gas Discharge Application for Fuel Ignition in a Jet Engine," K. Khodataev, A. Ershov, Proceedings of the 2nd Weakly Ionized Gas Workshop, Norfolk, April, 1998.
73. "Experimental and Theoretical Research and Optimization of Prospective Plasma Systems of Fuel Ignition in a Ramjet," I. Timofeev, Milestone 1, Task 1, JHU/APL Subcontract 808713, July 1999.
74. "Investigation of the Undercritical Microwave Discharge for Jet Fuel Ignition," I. I. Esakov, L. P. Grachev, K. V. Khodataev, and D. M. Van Wie, AIAA-2001-2939, June 2001.
75. "Experiments on Propane Ignition in High-Speed Air Flow Using a Deeply Undercritical Microwave Discharge," I. I. Esakov, L. P. Grachev, K. V. Khodataev, and D. M. Van Wie, AIAA-2004-0840, Jan. 2004.

76. “Experimental and Theoretical Research and Optimization of Prospective Plasma Systems of Fuel Ignition in a Ramjet,” I. Timofeev, Milestone 6, Task 2, JHU/APL Subcontract 808713, November 2000.
77. “Mechanisms of Transversal Electric Discharge Sustainment in Supersonic Air and Propane-Air Flows,” A. P. Ershov, N. V. Arvelyan, V. L. Bychkov, V. A. Chernikov, V. M. Shibkov, O. S. Surkont and I. B. Timofeev, AIAA-2003-0872, Jan. 2003.
78. “Superfast Homogeneous Plasma Ignition of Hydrogen-Oxygen and Air-Fuel Supersonic Flows by High Voltage Ionization Wave,” A. Yu. Starikovskii, Moscow Institute of Physics and Technology, April 2000.
79. “Combustible Mixture Ignition in a Wide Pressure Range. Nanosecond High-Voltage Discharge Ignition,” S. M. Bozhenkov, S. M. Starikovskaia, V. A. Sechenov, A. Yu. Starikovskii, V. P. Zhukov, AIAA-2003-0876, Jan. 2003.
80. “Hydrocarbon Fuel Ignition in Separation Zone of High-Speed Duct by Discharge Plasma,” S. Leonov, V. Biturin, K. Savelkin, D. Yarantsev, D. Van Wie, Fourth Workshop on Magnetoplasma Aerodynamics, Moscow, April 2002.

Table 1 – Sample power generation mass estimates.

	5 MW		100 MW	
	Access-to-Space	Cruise	Access-to-Space	Cruise
Auxillary MHD Power Unit	4.32 Ton	28.75 Ton	54.9 Ton	343.5 Ton
Inlet MHD Power Unit	1.25 Ton	5.87 Ton	25.0 Ton	117.4 Ton

Table 2. Comparison of virtual cowl with and without energy extraction and effect of energy deposition in combustor.

Case	Freestream Mach Number	Virtual Cowl with Energy Extraction		Virtual Cowl without Energy Extraction		No Virtual Cowl and Energy Addition	
		ΔC_T	ΔIsp	ΔC_T	ΔIsp	ΔC_T	ΔIsp
A	8	+6.8%	-0.27%	+7.6%	+0.46%	+0.78%	+0.78%
B	8	+10.5%	-0.82%	+12.0%	+0.57%	+1.48%	+1.48%
C	6	+8.0%	+0.20%	+8.7%	+0.78%	+0.63%	+0.63%
D	6	+14.0%	+0.05%	+15.1%	+1.10%	+1.18%	+1.18%
E	6	+15.8%	+0.27%	+17.0%	+1.30%	+1.18%	+1.18%
F	6	+33.6%	-0.52%	+37.2%	+2.17%	+3.50%	+3.50%

Table 3 – Potential drag reduction power savings.

Mach Number	Dynamic Pressure (psf)	Velocity (m/s)	Drag Reduction (N)	Drag Power Savings (MW)
6	1000	1798	26,869	48.0
8	“	2418	“	64.5
10	“	3063	“	81.8
6	2000	1780	53,378	95.0
8	“	2393	“	127.8
10	“	3028	“	161.6

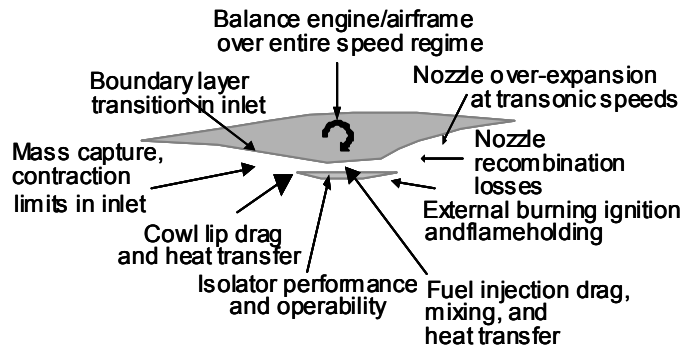


Figure 1 - Principal design issues of conventional space access vehicle employing airbreathing engines.

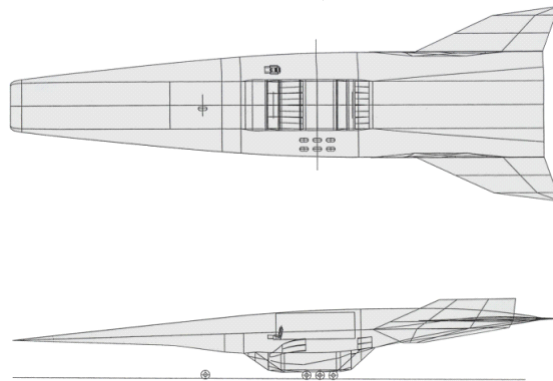


Figure 2 – Dual mission TSTO or hypersonic cruise aircraft.

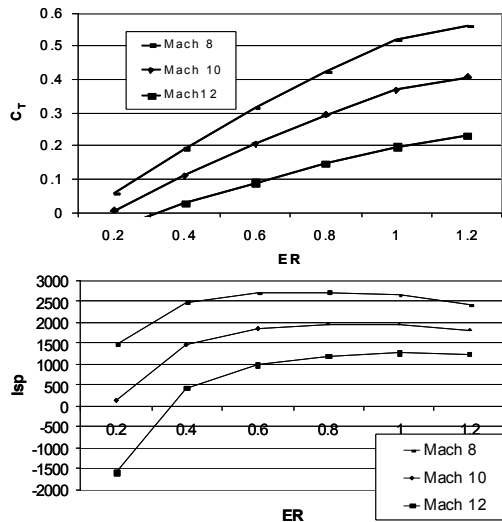


Figure 3– Baseline engine performance for Mach 10 class engine.

<p>Low-High MHD Inlet Flow Control</p>		<ul style="list-style-type: none"> • Design inlet for Mach 5 • MHD shock position control for $M > 5$ • Increase captured airflow $5 < M < 10$
<p>High-Low MHD Inlet Flow Control</p>		<ul style="list-style-type: none"> • Design inlet for Mach 10 • MHD compression for $M < 10$ • Increased captured airflow $5 < M < 10$
<p>Shock-Wave/Boundary-Layer Interaction Control</p>		<ul style="list-style-type: none"> • MHD separation control • Allow violation of weak-shock limit • Increased captured airflow $5 < M < 10$
<p>Virtual Cowl</p>		<p>Energy deposition to divert flow into engine</p> <ul style="list-style-type: none"> • Increased mass flow $5 < M < 10$

Figure 4– Techniques aimed at increasing engine thrust.

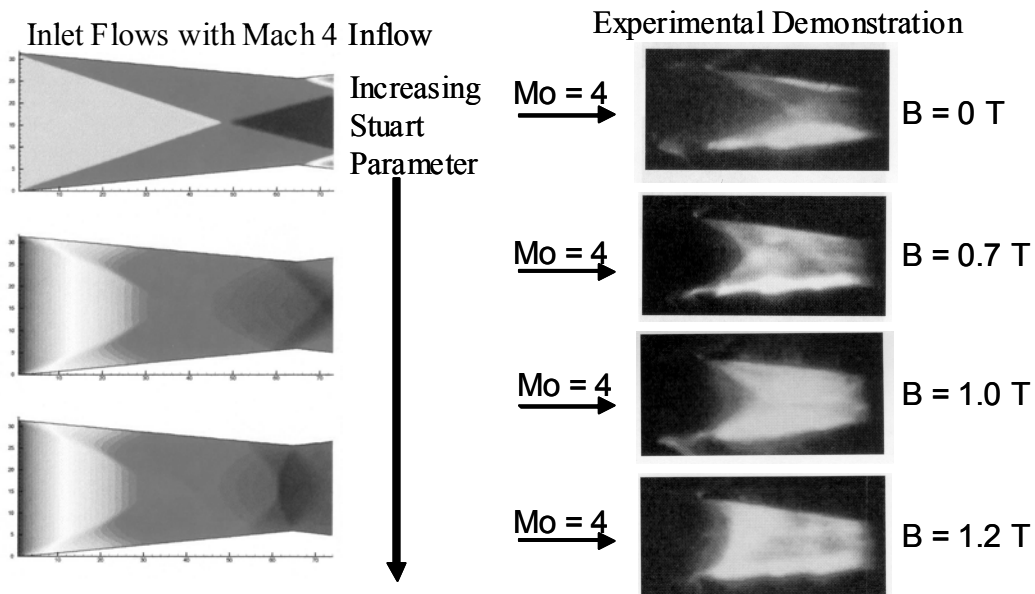


Figure 5 – Demonstration of MHD control of inlets Ioffe Institute.

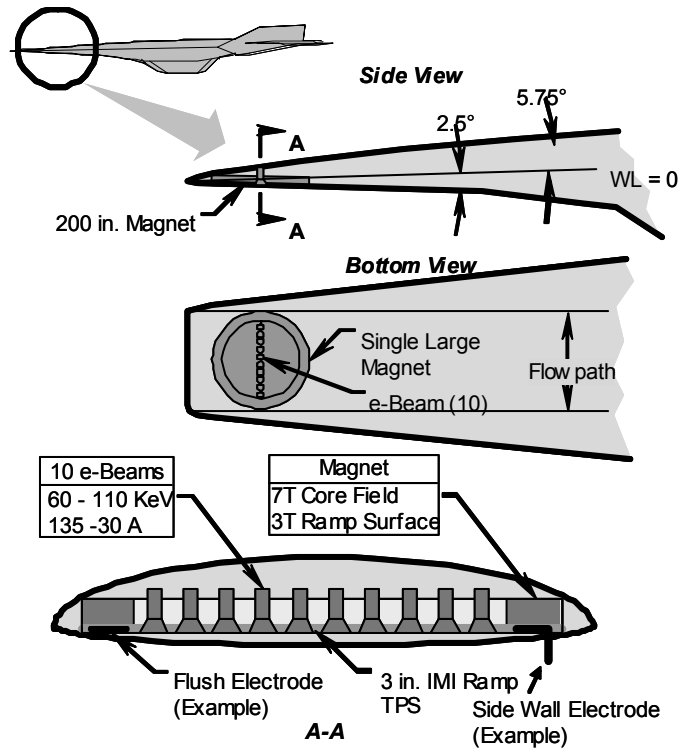


Figure 6– MHD inlet control system.

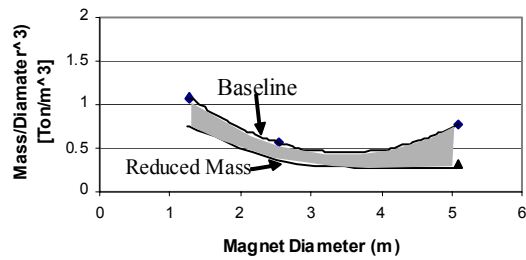
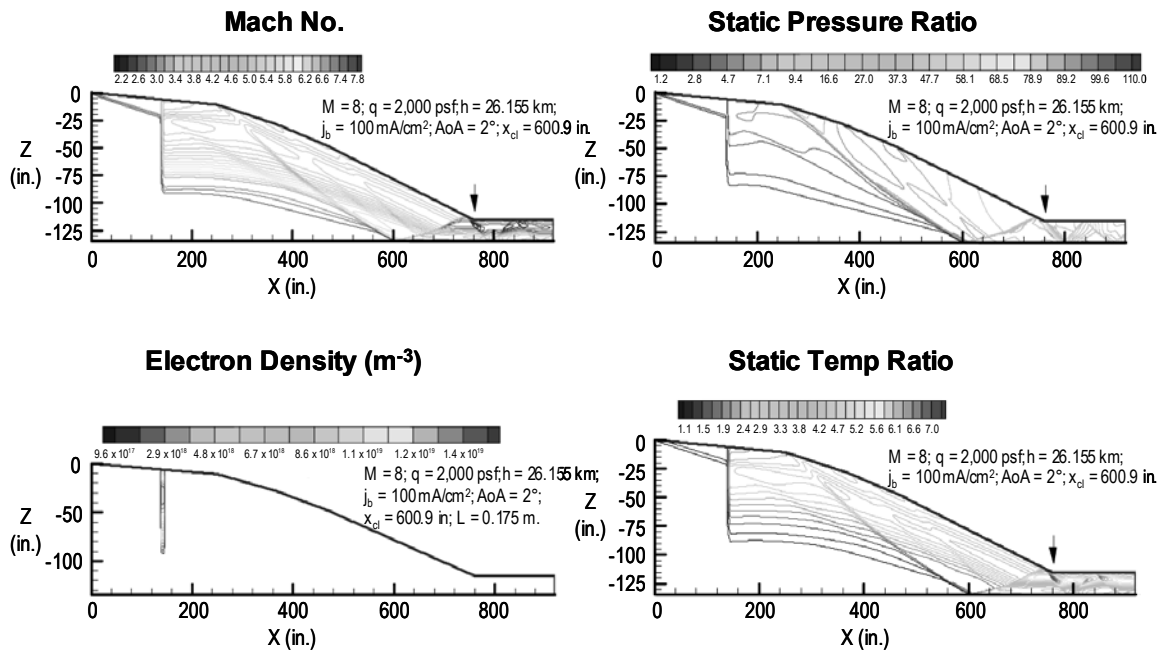


Figure 7 – Magnet mass model.



Aero Parameter at Throat Plane		MHD Parameter	
MFR	1.133	Pwr Extr (MW/m)	23.83
Pt Ratio	0.2	jxB Pwr (MW/m)	47.659
Ht Ratio	0.9843	Joule Htg (MW/m)	19.445
P Ratio	40.84	Pwr in Vibr Temp (MW/m)	4.384
Rho Ratio	9.077	e-Beam Pwr (MW/m)	13.6
T Ratio	4.5	Q*	0.09326
Eta-KE-Adiab	0.9563	%H ₀ Extract	2.435
Eta-KE-Cool	0.9394		
Mthrt	3.17		
Capt Ht (W/m)	9.454 x 10 ⁸		

Figure 8 – Predicted flowfield of MHD-controlled M_{DES}=10 inlet operating at Mach 8.

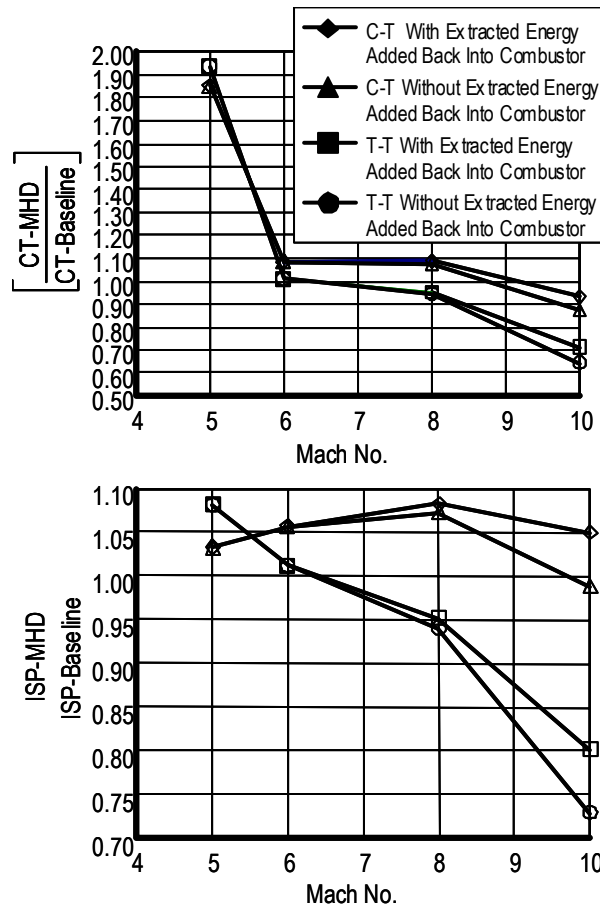


Figure 9– Effect of MHD-controlled in let on engine thrust and specific impulse characteristics,

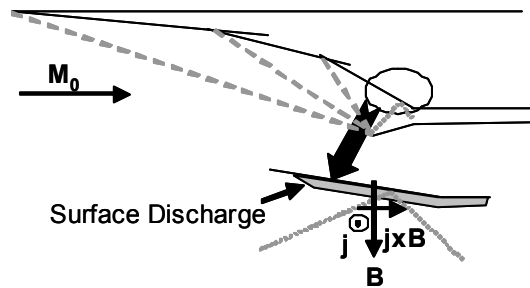


Figure 10 – Local MHD flow control for shock-wave/boundary-layer interaction control.

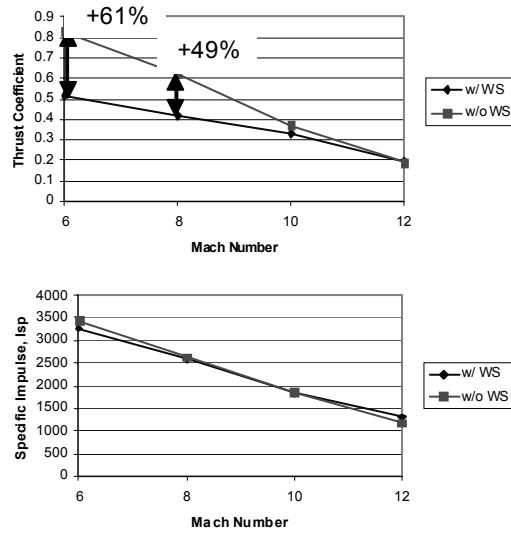


Figure 11 – Effect of shock-wave/boundary-layer interaction control on engine thrust and specific impulse characteristics.

Homogeneous Volume Discharges for Drag Reduction		<ul style="list-style-type: none"> Uniform energy deposition for flowfield modification
Heterogeneous Volume Discharges for Drag Reduction/Normal Force Modification		<ul style="list-style-type: none"> Nonuniform energy deposition for flowfield modification
Surface Discharges for Skin Friction Reduction		<ul style="list-style-type: none"> Energy deposition near surface for BL modification
Plasma Jet Injection for Drag Reduction		<ul style="list-style-type: none"> Jet interaction for flowfield modification

Figure 12 – Techniques at altering axial and normal forces.

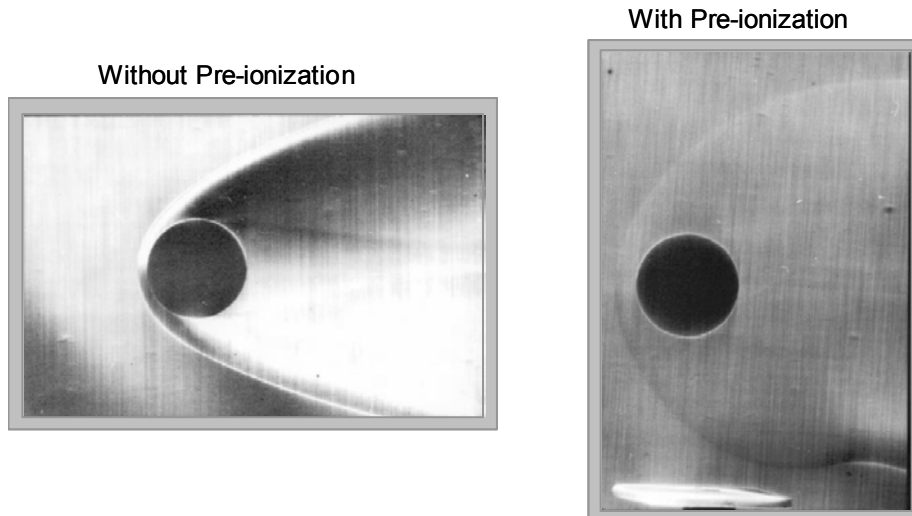


Figure 13 - Ioffe Institute Ballistic Range Tests Showing Effects of Ionization
Velocity = 2000 m/s

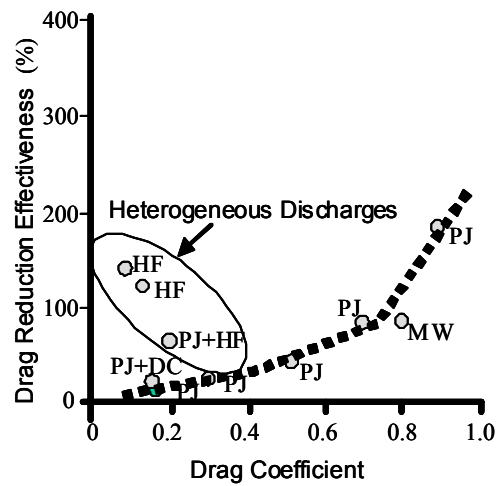


Figure 14- Drag reduction effectiveness for heterogeneous discharges (Ref. 36).

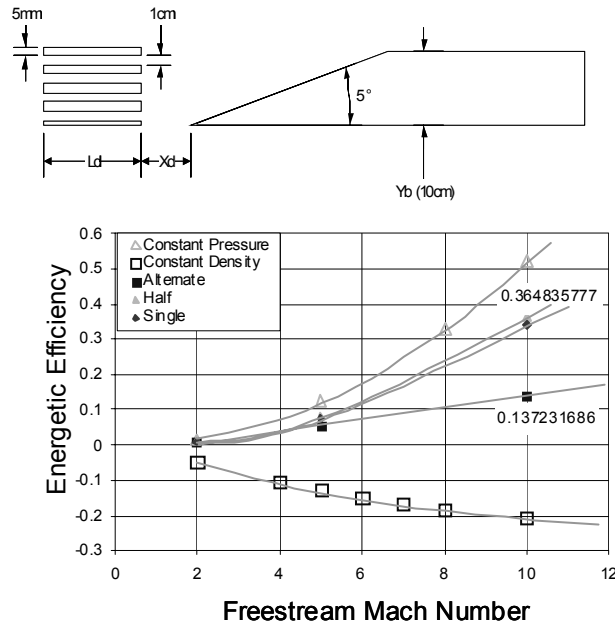


Figure 15 – Two-dimensional calculations of the effect of filamentary discharges on the drag reduction energetic efficiency of a 5° wedge.



% Viscous Drag Reduction	Viscous Drag Savings (N)	Drag Power Savings (MW)	Power Required (MW)		
			Effectiveness		
			0.2	1	2
0	0	0	0	0	0
10	8006.8	24.5	122.6	24.5	12.3
20	16013.5	49.1	245.3	49.1	24.5
30	24020.3	73.6	367.9	73.6	36.8
40	32027.0	98.1	490.6	98.1	49.1
50	40033.8	122.6	613.2	122.6	61.3

Figure 16– Skin friction reduction system.

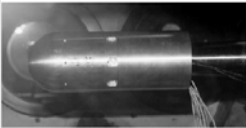
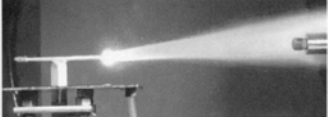
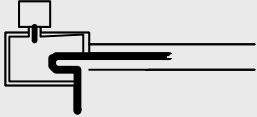
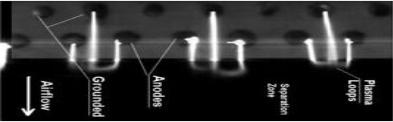
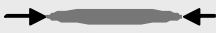
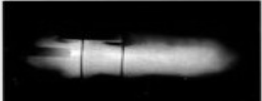
MHD Induced Heat Transfer Reduction at Leading Edges	
Subcritical Microwave Ignition and Flameholding	
Microwave Torch Ignition and Flameholding	
Pulsed DC Discharge Ignition and Flameholding	
Fast Ionization Wave Ignition and Flameholding	
Plasmadynamic Ignition and Flameholding	

Figure 17 – Techniques aimed at increasing operability.

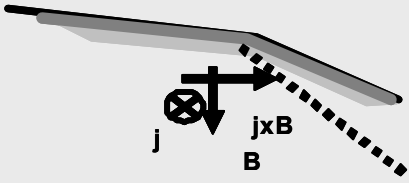
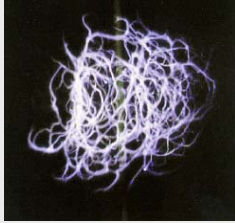
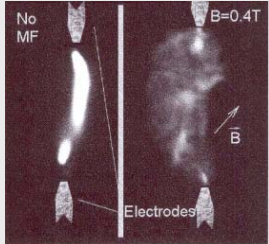
Inlet Laminar Flow Control	
Plasma Assisted Mixing with Heterogeneous Discharge	
Plasma Assisted Mixing with MHD Augmentation	

Figure 18 – Techniques aimed at increasing engine performance.

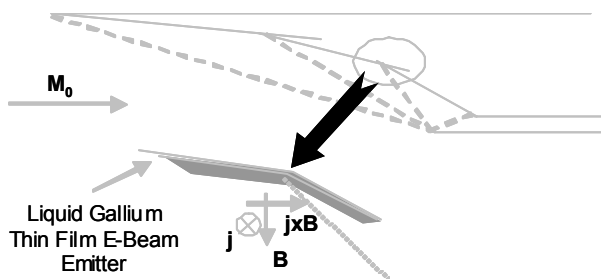


Figure 19 – Hypersonic inlet laminar flow control system.

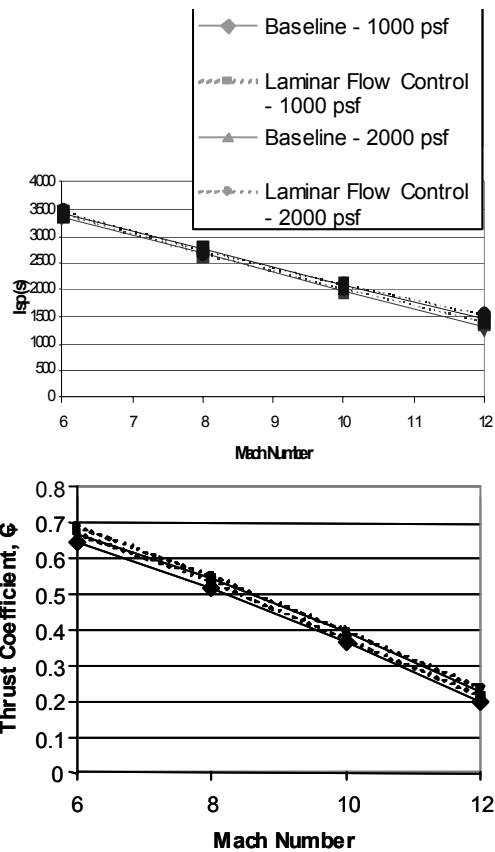


Figure 20 – Potential engine performance improvements from laminar-flow control system.